Article citation info:
Ouamara D, Boukhnifer M, Chaibet A, Maidi A. Diagnosis of ITSC fault in the electrical vehicle powertrain system through signal processing analysis. Diagnostyka. 2023;24(1):2023113. https://doi.org/10.29354/diag/161309.

DIAGNOSTYKA, 2023, Vol. 24, No. 1

e-ISSN 2449-5220
DOI: 10.29354/diag/161309

DIAGNOSIS OF ITSC FAULT IN THE ELECTRICAL VEHICLE POWERTRAIN SYSTEM THROUGH SIGNAL PROCESSING ANALYSIS

Dehbia OUAMARA [1,*], Moussa BOUKHNIFER [2], Ahmed CHAIBET [3], Ahmed MAIDI [4]

[1] Department of Electrotechnics, Mouloud Mammeri University of Tizi Ouzou, Algeria
[2] University of Lorraine, LCOMS, F-57000 Metz, France
[3] ISAT, University of Burgundy, France
[4] L2CSP Laboratory, Mouloud Mammeri University of Tizi Ouzou, Algeria
[*] Corresponding author, e-mail: dehbia.ouamara@ummto.dz

Abstract

The three-phase induction motor is well suited for a wide range of mobile drives, specifically for electric vehicle powertrain. During the entire life cycle of the electric motor, some types of failures can occur, with stator winding failure being the most common. The impact of this failure must be considered from the incipient as it can affect the performance of the motor, especially for electrically powered vehicle application. In this paper, the intern turn short circuit of the stator winding was studied using Fast Fourier transform (FFT) and Shor-Time Fourier transform (STFT) approaches. The residuals current between the estimated currents provided by the extended Kalman filter (EKF) and the actual ones are used for fault diagnosis and identification. Through FFT, the residual spectrum is sensitive to faults and gives the extraction of inter-turn short circuit (ITSC) related frequencies in the phase winding. In addition, the FFT is used to obtain information about when and where the ITSC appears in the phase winding. Indeed, the results allow to know the faulty phase, to estimate the fault rate and the fault occurrence frequency as well as their appearance time.

Keywords: Induction motor, electrical vehicle, fault diagnosis, inter-turn short circuit, extended Kalman filter, spectral analysis, Fast Fourier transform, Short –Time Fourier transform.

1. INTRODUCTION

The need to reduce global warming, as a result of the Paris Agreement, the need for countries to achieve climate neutrality in the second half of the 21^{st} century has led to changes. One of these changes is certain ambitions such as reducing greenhouse gas emissions (GHGs), carbon dioxide (CO_2) emissions, fuel consumption and other pollutants and diversifying the energy sources used [1,2,3]. Electrical Vehicle (EV) technology is among the promising solution for achieving some of these ambitions. Indeed, efforts are underway in a number of countries to boost the number of EVs in order to achieve the decarbonisation of the transportation sector [4, 5].

A common electric vehicle system consists mainly of three components: an electric drive train, a controller and power supply. The advancement and development of the electric vehicle are strictly linked to its electric drive train, and more specifically to the kind of electric motor involved. Popular motors for EVs applications are permanent magnet synchronous machines (PMSMs) or induction motors (IMs). The high expense of PMSMs, as well as their moderate power density render them less appealing for EVs use. In contrast, the robustness over a wide speed range, simple to control, low maintenance cost, low price, small size and lightweight of induction motors make them an attractive choice for numerous EVs applications [6, 7].

However, due to long term continuous operation or operating conditions, faults such as electrical, mechanical and magnetical faults can occur in the motor [8]. The short circuit fault in stator winding is the more common fault occurring in induction motors, accounting for approximately 38% of all faults [9]. The short circuit fault can cause serious problems in the electrical vehicle, it affects the reliability and motor operating safety, when it occurs a high circulating current and high heat are generated in the fault circuit [10, 11].

Early diagnosis of short circuits in induction motors is a crucial issue to correct the fault in time and avoid any damage. Considerable research and development efforts are devoted to ensuring vehicle performance and safety to avoid damage caused by faults, affecting the reliability and continuous operation of the drive system.

For the development of an efficient diagnosis system, the main point is the identification of the

changes in the motor performance and behaviour induced by a fault. Usually, currents are used for fault diagnosis. However, there are methods that are based on other parameters like electromagnetic torque [12, 13], vibration signal [14] and mechanical speed [15].

Most studies focus on current analysis to detect inter turns short circuit fault in the stator winding. In [16], discrete wavelet transform is designed to analyse the currents to detect the ITSC in the first time and estimate the number of defective turns in faulty phase. FFT and fuzzy logic are applied in [17] based on the stator currents to detect the shorted phase winding. It is shown that the fuzzy logic is better than the total harmonic distortion when the faults currents is distorted. A linear inter-turn short circuit separation ITSC in a three-phase induction motor to identify short circuit is conducted in [18]. The authors noted through an analysis of the relationship between inductance and number of windings, that the current decreased slightly in the ITSC.

However, there are few studies that have addressed this type of fault using the extended Kalman filter. Khayam Hoseini et al. [19] suggested a fault detection technique based on the difference between the estimated resistance and the normal condition resistance (residual signal) in Switched reluctance motors (SRMs) using EKF. IT is ascertained that the value of this ascertained residual signal can be utilized as an effective index for inter-turn fault detection. An EKF and UKF used for fault detection and isolation of stator windings in permeant magnet synchronous generator (PMSGs) [20]. The resulting gains were outlined as fast and precise response compared to the time required to act in real time and robust estimation in the presence of process and measurement noise.

This paper deals with the frequency analysis of the residual between the estimated currents by EKF and the actual currents, which allows to know the faulty phase and the frequency signature clearly. We have not encountered studies similar to ours.

We applied the FFT to the stator currents for different short circuit rates to extract the frequency signatures related to the inter-turn short circuit fault. In order to improve our study, an Extended Kalman filter (EKF) is designed. A frequency study of the residual signals between the estimated currents by the EKF and the real currents was performed for different short circuit rates both without load and with the load.

The FFT approach has some limitations because it provides only frequency data. To know the fault occurrence time, which is important in such an investigation, the Short–Time Fourier transform (STFT) is used to overcome this limitation. STFT displays a double dimensional window: frequency and time information. In addition, it yields the location of the fault in time while capturing the frequency information simultaneously [21].

This paper is organized as follows: Section 2 presents both the behavior of induction motor, with inter turn short circuit, and the FFT current analysis. In section 3, an EKF is designed to estimate the states variables and the residuals analysis by FFT performed. Section 4 is devoted to STFT residual analysis results. Finally, some concluding remarks are given in section 5.

2. INDUCTION MACHINE MODELING WITH INTER-TURN SHORT CIRCUIT FAULT AND ITS IMPACTS

2.1. Induction machine model with inter turn short circuit faults

The short circuit stator's fault in induction motor can be modelled as a new winding added to the stator's healthy winding, it depends by two parameters. This new winding has two parameters, which can give information about the location and ratio of the winding. Figure 1 illustrates an inter turns short circuits scheme of induction motor.

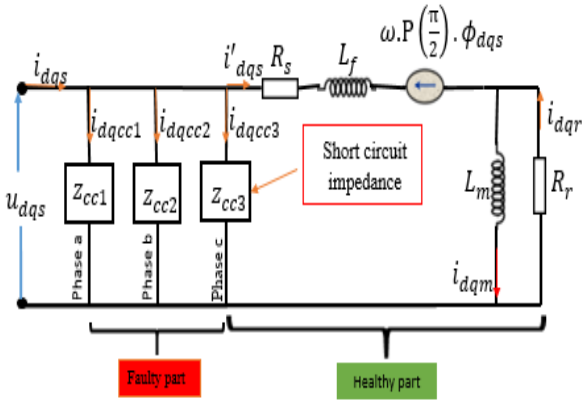

Fig. 1. Scheme of the inter-turn short circuit fault stator in induction motor [19]

The mathematical model under inter turn short circuit in dq reference frame are given by following equations [22, 23]:

$$\begin{cases} \dot{x}(t) = A(\Omega)x(t) + Bu(t) \\ y(t) = Cx(t) + F(t)u(t) \end{cases} \quad (1)$$

Where $x = [i_{ds},\ i_{qs},\ \varphi_{dr},\ \varphi_{qr}]^T$ is the state variable with, i_{ds} and i_{qs} are the stator currents, φ_{dr} and φ_{qr} are the rotor fluxes.

$y = [i_{sd} \quad i_{sq}]^T$ are the vector of the measurable outputs.

The matrices involved in model (1) are defined as follows

$$A = \begin{bmatrix} -\varsigma & \omega_s & \frac{K}{\tau_r} & P\Omega K \\ -\omega_s & -\varsigma & -P\Omega K & \frac{K}{\tau_r} \\ \frac{M_{sr}}{\tau_r} & 0 & \frac{-1}{\tau_r} & \omega_s - P\Omega K \\ 0 & \frac{M_{sr}}{\tau_r} & -(\omega_s + P\Omega K) & -\frac{1}{\tau_r} \end{bmatrix} \quad (2)$$

$$B = \begin{bmatrix} \frac{1}{\sigma L_s} & 0 \\ 0 & \frac{1}{\sigma L_s} \\ 0 & 0 \\ 0 & 0 \end{bmatrix} \quad (3)$$

$$C = \begin{bmatrix} 1 & 0 & 0 & 0 \\ 0 & 1 & 0 & 0 \end{bmatrix} \quad (4)$$

The mechanical speed Ω is the sollution of the following equation

$$J\frac{d\Omega}{dt} = C_{em} - C_r - k_f\Omega \quad (5)$$

with

$$C_{em} = M_{sr}\left(i_{ds}i_{dr} - i_{ds}i_{qr}\right) \quad (6)$$

Where M_{sr} is the mutual inductance (stator-rotor), R_r and R_s are the stator and rotor resistance, respectively. L_s and L_r are the stator and rotor inductance, respectively. C_{em} is the electromagnetic torque, C_r the load torque, J is inertia moment and k_f is friction coefficient. The different parameters are given as follows

$$\sigma = 1 - \frac{{M_{sr}}^2}{L_s L_r}$$

$\tau_s = \frac{R_S}{L_S}$ is the stator time constant

$\tau_r = \frac{R_r}{L_r}$ is the rotor time constant

$\varsigma = -\frac{1}{\sigma\tau_s} - \frac{1-\sigma}{\sigma\tau_r}$.

The matrix F is given by:

$$F(\varpi(-\theta), \eta_{cck'}) = \frac{2}{3*R_S}\sum_{k'=1}^{3}\eta_{cck'}P(-\theta)\varpi(-\theta_{cck'})P(\theta) \quad (7)$$

$$\boldsymbol{\eta_{cck'}} = \frac{N_{cc}}{N_s} = \frac{Number\ of\ interturns\ short-circuit\ \ winding}{Total\ number\ of interturns\ in\ one\ phase} \quad (8)$$

$$P(\theta) = \begin{bmatrix} cos(\theta) & -sin(\theta) \\ sin(\theta) & cos(\theta) \end{bmatrix} \quad (9)$$

$$\varpi(\theta_{cck'}) = \begin{bmatrix} \cos(\theta_{cck'})^2 & \cos(\theta_{cck'})\sin(\theta_{cck'}) \\ \cos(\theta_{cck'})\sin(\theta_{cck'}) & \sin(\theta_{cck'})^2 \end{bmatrix} \quad (10)$$

Where: $P(\theta)$ is the park rotational matrix and $\theta_{cck'}$ is the reel angle between the defective stator winding and the first stator phase axis. This parameter can take three values $0, \frac{2\pi}{3}$ and $\frac{4\pi}{3}$ that allow to locate the interturns short-circuit , respectively, in phase a, b and c. k' indicates one of the three stator phases.

The short circuit currents are given by:

$$\begin{bmatrix} i_{dscc} \\ i_{qscc} \end{bmatrix} = F\begin{bmatrix} v_{ds} \\ v_{qs} \end{bmatrix} \quad (11)$$

The short circuit currents can be written as follows:

$$\begin{bmatrix} i_{dscc} \\ i_{qscc} \end{bmatrix} = \frac{2}{3R_s}\sum_{k'=1}^{3}\boldsymbol{\eta_{cck'}P(-\theta)\varpi(-\theta_{cck'})P(\theta)}\begin{bmatrix} v_{ds} \\ v_{qs} \end{bmatrix} \quad (12)$$

Consequently, the resultant dq stator currents are expressed as follows:

$$\begin{bmatrix} i_{dsf} \\ i_{qsf} \end{bmatrix} = \begin{bmatrix} i_{ds} \\ i_{qs} \end{bmatrix} + \begin{bmatrix} i_{dscc} \\ i_{qscc} \end{bmatrix} \quad (13)$$

Where i_{ds} and i_{qs} are the stator current passing through the healthy winding. Therefore, for a healthy stator winding, the parameter $\eta_{cck'}$ $(\eta_{cck'} = \frac{N_{cc}}{N_s})$ equal to zero because N_{cc} takes a zero value.

2.2. Analysis of the impact of inter turn short circuit on induction machine using FOC control

To date, few attempts have made to investigate the fault diagnosis of induction motor in closed loop system. This is, due principally to the fact that the controller modifies the impact of damage compared to the open loop [24].

Figure 2 gives the simulation results of the induction motor with the field-oriented control (FOC). It can be seen that in healthy regime, the stator currents are sinusoidal and have the same amplitude. But in the presence of the inter-turns short circuit on the phase a at time interval t_1 (1.5 s-1.8 s) without load and at time interval t_2 (2.5s-2.8s) with load, there will be an imbalance at the level of the stator currents which increase in term of amplitude. It can conclude that the short circuit affects the faulty phase, that is the phase a compared to the other phases which are less impacted. Also, we observe the influence of inter turns short circuit on the other machine variables. When the inter- turns short circuit occurs, important oscillations are observed in the electromagnetic torque. Consequently, a perturbation of the mechanical speed is not very important, which be explain by the fact that the Proportional and Integral (PI) speed controller behave well by minimizing the effects of INTSC fault on the speed.

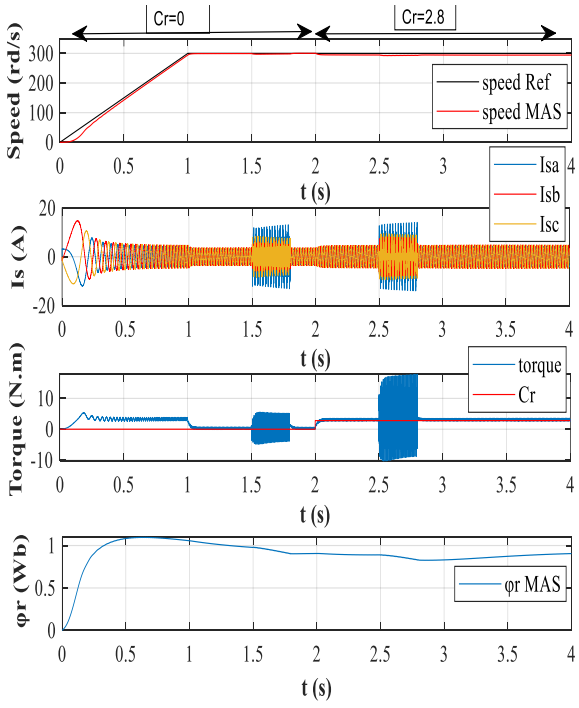

Fig. 2. Simulation results of induction motor in healthy case and in presence of inter turns short circuit of 10% given at times intervals t_1 and t_2.

Now, we apply the FFT to the stator currents in order to extract the signature analysis frequencies in healthy case and in the presence of short circuit inter turns on phase a. The simulation results are given by Figure 3, show clearly the appearance of a single frequency at 50 Hz in healthy mode, which is the fundamental frequency of the motor. However, in the presence of inter-turns short circuit fault, other frequencies appear at 150 Hz and at 250 Hz. These frequencies that occur after the application of the short-circuit fault inter turns are very cited in the literature. Theoretically, the harmonic frequency of the induced current when the short circuit fault occurs in the stator is given by the equation (14) [25].

$$f_{ITSC} = \left[\frac{n'}{p}(1-s) \pm k''\right] f_S \tag{14}$$

n'=1,2,3….; k''=1,3,5….; p is pole pair

f_S is fundamental frequency of stator current and, s is the slip;

The spectrum amplitude of three stator currents in the presence of different short circuit rates is illustrated in the same Figure. We observe that the inter-turns short circuit generates the appearance of 3rd and 5th harmonic of the fundamental component. The amplitude of the fundamental harmonic increases proportionally to the short circuit rate. The same remark is made to the 3rd harmonic, but for the 5th harmonic amplitude is very small, which is about 10^{-2}.

According to the equation (14) we obtain the same frequencies in our simulation when we inject the ITSC fault in phase a in the stator winding.

3. EXTENDED KALMAN FILTER (EKF)

Extended Kalman Filter is the most suitable observer to estimate the state variables of a nonlinear system [4- 26- 27]. EKF is robust against measurements noises and modelling errors [29]. We have designed an EKF to estimate the variable state of the induction motor. We use the discrete model of induction motor in fixed reference frame α, β with five state variables. The discrete model is given by the following equations [30,31]:

$$x_{k+1} = A_k x_k + Bu_k + w \tag{15}$$

$$y_k = Hx_k + v \tag{16}$$

$$\begin{cases} w \cong N(0,Q) \\ v \cong N(0,R) \end{cases} \tag{17}$$

Where, $i_{s\alpha}$ and $i_{s\beta}$ are the stator currents, $\varphi_{r\alpha}$ and $\varphi_{r\beta}$ are the rotor fluxes, Ω is the mechanical speed of the motor, L_s and L_r are respectively the stator and rotor inductances, R_s and R_r are respectively the stator and rotor resistances, T_e is the sample time.

w and v are process and measurement noise with zero mean and covariance matrix Q and R, respectively, given in APPENDIX A.

The EKF is based on three main steps. The first one is the prediction step that uses the estimated state of the previous moment to estimate the actual current state. The second step consists in predicting of parameter P_k^p and the computation of the Kalman filter gain K_k . The last step is the determination of the final value of the state vector in the correction step. These steps are summarized by the following equations:

Prediction:

$$x_k^p = A_k \hat{x}_{k-1} + Bu_{k-1} \tag{18}$$

$$P_k^p = A_k P_{k-1} {A_k}^T + Q$$

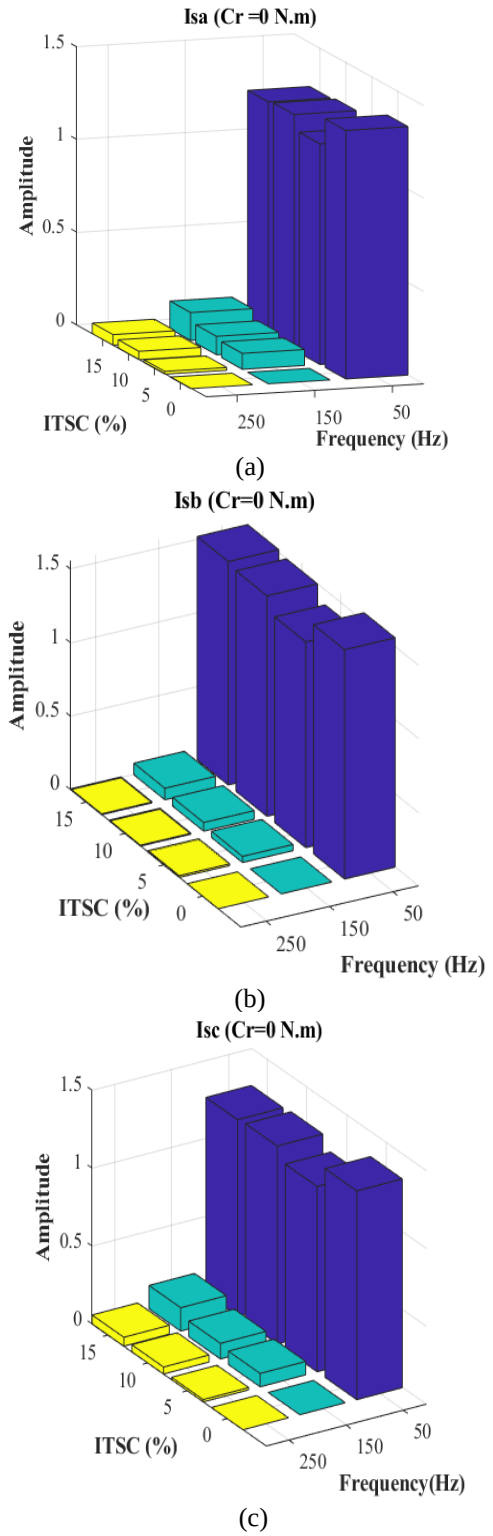

Fig. 3. Stator currents spectrum in the presence of different inter turns short circuit

Gain computation: $K_k = P_k^p H^T \left(H P_k^p H^T + R\right)^{-1}$ (19)

Update: $\hat{x}_k = x_k^p + K_k\left(y_k - H x_k^p\right)$ (20)

$$\hat{P}_k = (1 - K_k H) P_k^p$$

where:

F and H are the Jacobeans of the state and measurements functions, respectively, which are given in the appendix A.

The simulation results obtained using the EKF given by the Figure 4. We notice that the estimated currents behave like the real currents, so the EKF is the most adapted to the estimation of the induction motor states.

According to the residual signals r, obtained in simulation between the real and the estimated currents shown in Figure 5, we can notice that the three residual signals of the three phases are around 3 % in transient and converge to 0 in steady state without fault, at intervals times t_1 (1.5 to 1.8s) and t_2 (2.5 to 2.8s). We observed a significant change of residual signals amplitude when the fault occurs. Due to these performances, the residual signals will be used for fault diagnosis inter turn short circuit in stator winding.

Figure 6 illustrates the generation residual signals r. The computed residual signals allow to detect the fault occurrence by comparing the residual signals to the threshold residual signals in healthy mode. When the residual signals are higher than threshold value, it means the presence of the fault. Then by processing the residual signal, the characteristics of the occurred fault are identified.

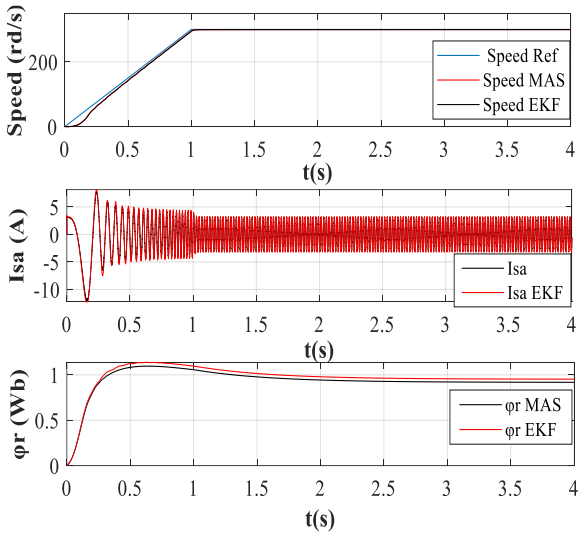

Fig. 4. Simulation results of the extended Kalman filter

Figures 7 and 8 show the spectrum amplitude of the three residual signals in different short circuit rates taking into account load torque (Cr=2.8N.m) in Figure 8 and without load torque (Cr=0N.m) in Figure 7. It is noticed that in healthy mode we can see only the fundamental harmonic at 50 Hz with a small amplitude of the residual signals. The occurrence of the ITSC fault in the induction motor in phase a increase the amplitude of the fundamental harmonic and leads to the occurrence of the 3rd harmonic, and the residual signals amplitude increase proportionally with the increasing short circuit rate. We note that the results are important in term of residual amplitude of the faulty phase compared to the other two phases, allowing us to identify the faulty phase and to estimate the short circuit rate.

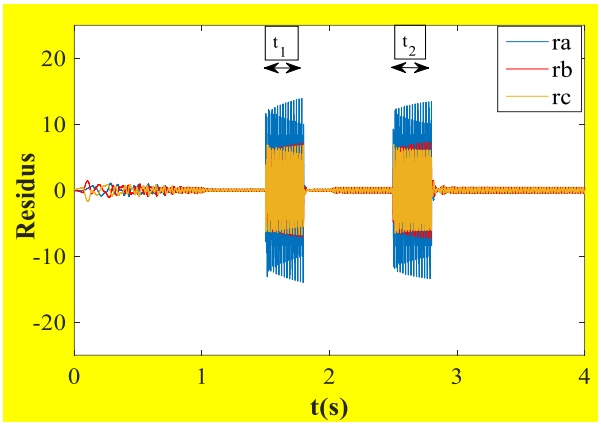

Fig. 5. Residuals simulation results

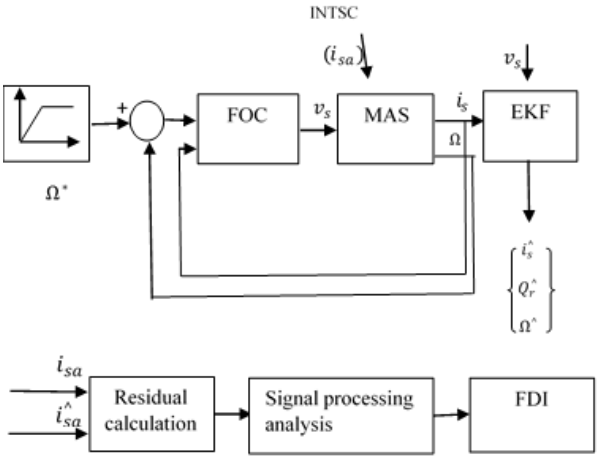

Fig. 6. Residual signal generation based on EKF and FDI scheme

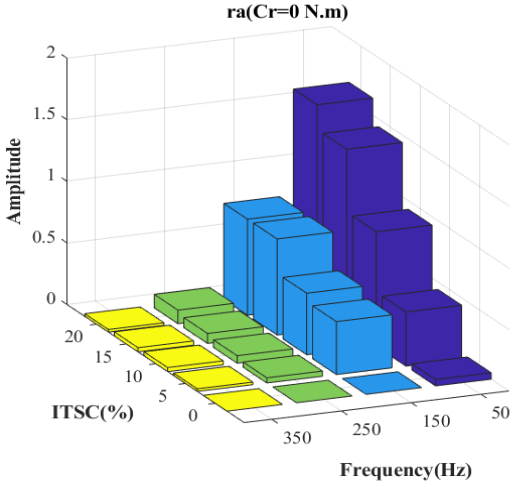

(a)

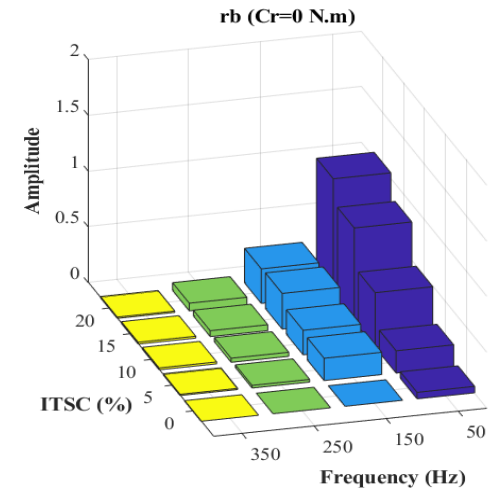

(b)

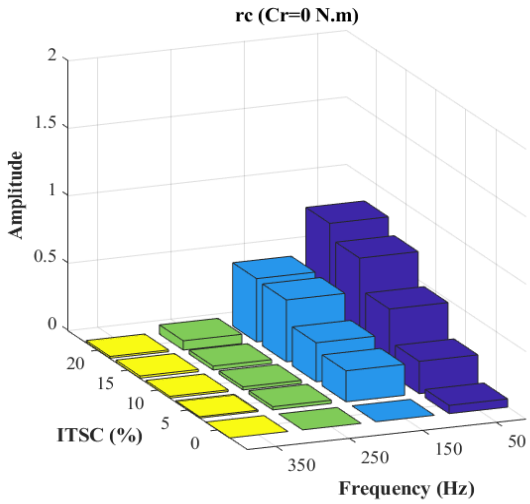

(c)

Fig. 7. Residual signals spectrum results in different ITSC in phase a without load

4. SHORT TIME FOURIER TRANSFORM ANALYSIS

The frequency domain given by the FFT analysis does not provide information on the time of occurrence of a particular frequency, despite the resolution provided is good. Moreover, the FFT is only effective in the case of a stationary signal. In the diagnosis of electrical faults, it is essential to get information on the appearance time of the fault, which allows to identify the source of the fault. STFT is an FFT extension in the time-frequency domain analysis, it overcomes the constraints of FFT analysis and well adapted to the analysis of non-stationary signals [32].

The STFT in continuous domain is given as follows [33].

$$S(t,f) = \int_{-\infty}^{+\infty} f(t)w(\tau - t)e^{-j2\pi f\tau}d\tau \qquad (21)$$

The signal is sampled at a fixed sampling frequency (fs), and the DFT is calculated to analyse the frequency spectrum by applying the fast Fourier transform (FFT) algorithm.

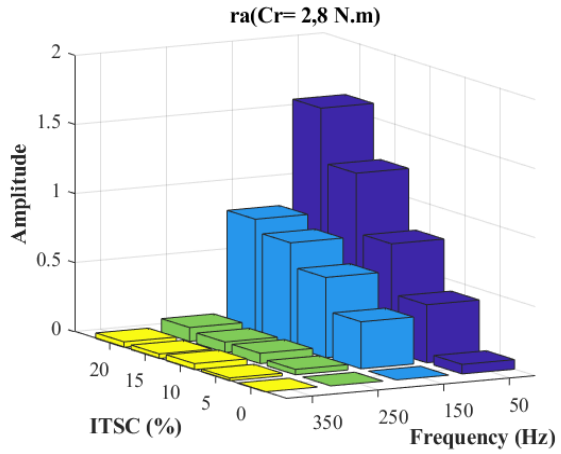

(a)

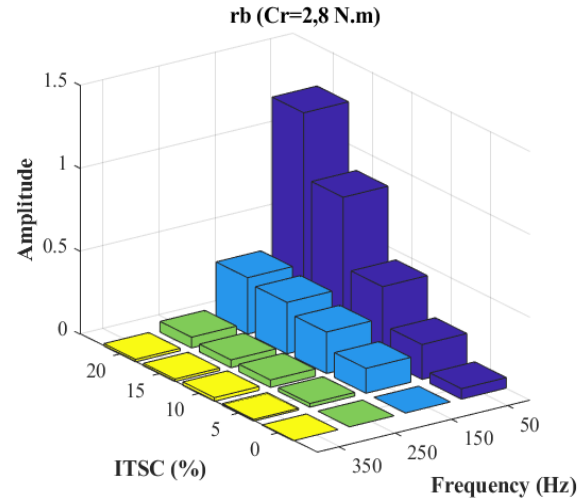

(b)

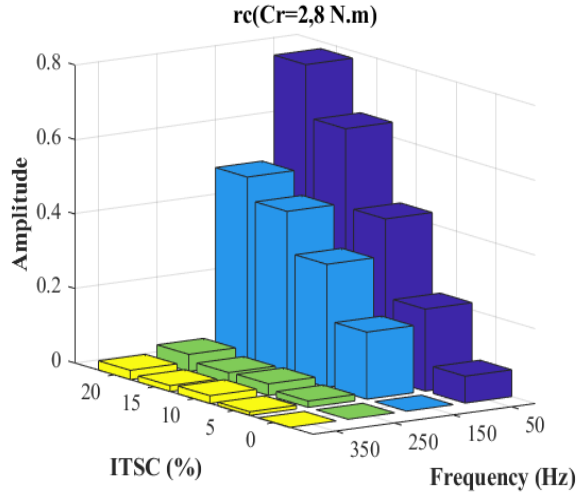

(c)

Fig. 8. Residual signals spectrum results in different ITSC in phase a with load

The STFT in the discrete domain is given as follows:

$$s[m,k_f] = \sum_{n=0}^{n=N-1} x[n]w[n-mH]e^{-j\frac{2\pi nk_f}{N}} \qquad (22)$$

Where: N the number of FFT points, $x[n]$ is the input sample, n is the time-domain input sample

index, k_f is frequency index, $w[n]$ is the window function and m is its position, H is the window size.

STFT depends on these parameters:

1) **Sampling frequency (fs)**: affects both the time and the frequency resolution of the STFT output. Higher fs results in better time and frequency resolution and vice versa. In this paper, fs of the STFT-based algorithm is limited to 10^4 kHz.
2) **Number of input sample (n):** It is the number of samples of the input signal on which the windowing function is applied.
3) **Type of the window function w[n]:** the most popular window functions available to carrying out STFT are Triangular, Rectangular, Bartlett, Hanning and Hamming. In this study, Hanning window is used.
4) **The window size (H)**: The window size is responsible for the STFT output resolution in time-domain. The better resolution of the time is the lower size of the window.

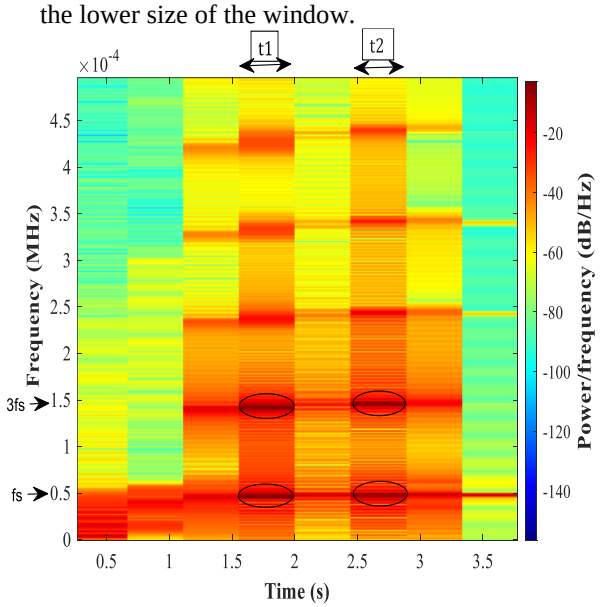

Fig. 9. STFT spectrogram of the residual ra in damaged and undamaged motor

From the results given by Figure 9, a momentary change in the frequency components fs and 3fs (dark color) are observed (the change are marked by the small circles in the ranges time t_1 (1.5 to 1.8s) and t_2 (2.5 to 2.8s) due to the presence of the short circuit fault of 10% of the total number of turns in the stator winding of phase a, while elsewhere this change does not appear.

In figure 10, we observed only the frequency of 50 Hz over the entire time range because there is no fault.

In Figure 11, a significant change is observed over the entire time range for the fundamental and third harmonic frequencies, while it is non-existent in the healthy case, indicate the presence of the fault over this entire time range. In addition, an increase in power/frequency is visible, which confirms the previous finding.

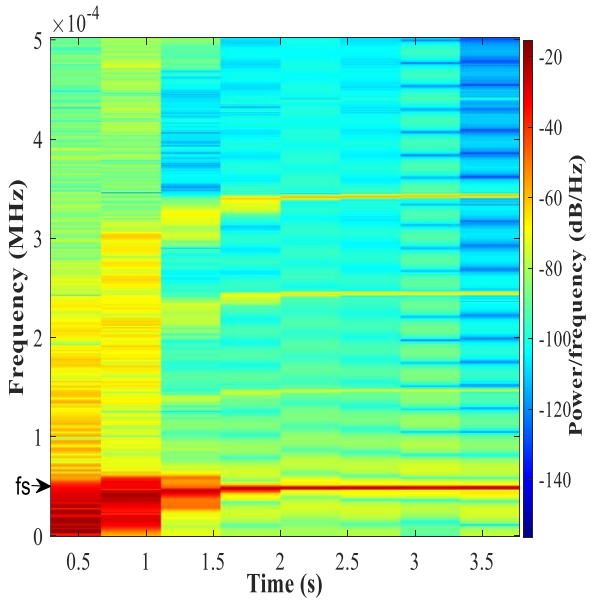

Fig. 10. STFT spectrogram of the residual ra in healthy case

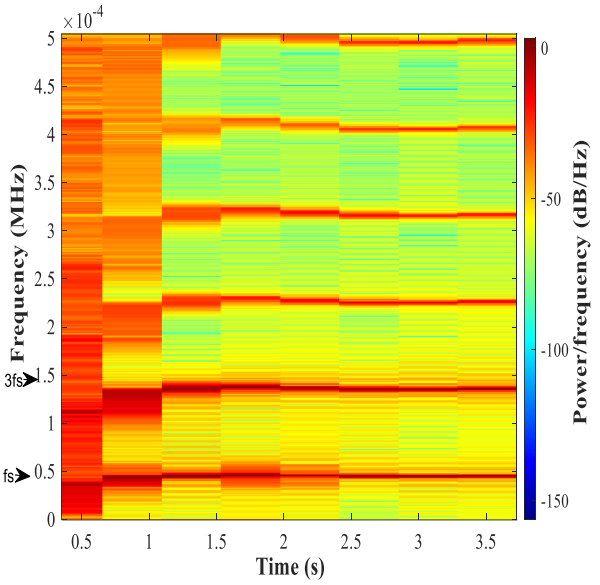

Fig. 11. STFT spectrogram of the residual ra in damaged motor (ITSC 10%).

In addition, harmonics insensitive to ITSC fault occur with low energy (power/frequency).

It is deduced that the most sensitive frequencies to the ITSC fault are the fs and 3fs frequencies where their power/frequency values for an undamaged and damaged motor differ significantly, making them a strong fault indicator.

To reveal the remarkable feature of STFT analysis, the ability of the proposed technique is to find the symptoms of the momentary short circuit and define the time of the short circuit fault.

5. CONCLUSION

This paper discusses the problem of inter-turn short circuit stator winding fault in an induction motor in the context of an electric vehicle application. Both FFT analysis and STFT analysis

are applied to the signal processing to extract the ITSC symptoms. The study was carried out for the stator phase current signal and expanded to the computed residuals between the stator currents estimated by the extended Kalman filter and the actual currents, which is a meaningful contribution to the topic of fault detection in induction motors.

The finding confirmed the effectiveness of the application of the STFT analysis on the residuals for retrieving ITSC fault characteristics in a stator phase compared to FFT analysis, which is also relevant for retrieving ITSC fault characteristics. The STFT-based method also enables the determination of the time of fault occurrence and the monitoring of the harmonic power/frequency in the drive system. Moreover, these results could be practical to apply in the process of evolution of automatic diagnostic systems, assisted by artificial intelligence, based on a suitable selection of fault characteristics.

Future work will be conducted on test bench.

Author contributions: *rresearch concept and design, D.O., M.B., A.C., A.M.; Collection and/or assembly of data, D.O., M.B., A.C., A.M.; Data analysis and interpretation; Writing the article, D.O.; Critical revision of the article, D.O., M.B., A.C., A.M.; Final approval of the article, (D.O., M.B., A.C., A.M.*

Declaration of competing interest: *The authors declare that they have no known competing financial interests or personal relationships that could have appeared to influence the work reported in this paper.*

APPENDIX A

This appendix presents the matrices and parameters used in the discrete model of the extended Kalman filter expressed in section 3.

The matrices used in equations (15) and (16) are defined as follows

Where $x_k = \begin{bmatrix} i_{s\alpha} \\ i_{s\beta} \\ \varphi_{r\alpha} \\ \varphi_{r\beta} \\ \Omega \end{bmatrix}$; $u_k = \begin{bmatrix} u_{s\alpha} \\ u_{s\beta} \end{bmatrix}$; $y_k = \begin{bmatrix} i_{s\alpha} \\ i_{s\beta} \end{bmatrix}$;

$$A_k = \frac{df(x,u)}{dx} = \begin{bmatrix} a_{11} & b_{11} & a_{12} & b_{12} & f_1 \\ -b_{11} & a_{11} & -b_{12} & a_{12} & f_2 \\ a_{21} & b_{21} & a_{22} & b_{22} & f_3 \\ -b_{21} & a_{21} & -b_{22} & a_{22} & f_4 \\ 0 & 0 & 0 & 0 & 1 \end{bmatrix}$$

$$B = \begin{bmatrix} a_1 & 0 \\ 0 & a_1 \\ a_2 & 0 \\ 0 & a_2 \\ 0 & 0 \end{bmatrix}$$

$$H = \begin{bmatrix} 1 & 0 & 0 & 0 & 0 \\ 0 & 1 & 0 & 0 & 0 \end{bmatrix}$$

The covariance matrices are defined as

$$Q = \begin{bmatrix} \delta_\varphi & 0 & 0 & 0 & 0 \\ 0 & \delta_\varphi & 0 & 0 & 0 \\ 0 & 0 & \delta_i & 0 & 0 \\ 0 & 0 & 0 & \delta_i & 0 \\ 0 & 0 & 0 & 0 & \delta_\Omega \end{bmatrix}$$

$$R = \begin{bmatrix} \delta_b & 0 \\ 0 & \delta_b \end{bmatrix}$$

The different parameters are given as follows

$$a_{11} = 1 + \alpha T_e + (\alpha^2 + \beta\gamma){T_e}^2/2$$

$$a_{12} = \beta T_e \left(1 + \frac{(\alpha+\beta)T_e}{2}\right) + c\Omega^2\, {T_e}^2/2$$

$$a_{21} = \gamma T_e \left(1 + \frac{(\alpha+\beta)T_e}{2}\right)$$

$$a_{22} = 1 + \delta T_e + \frac{(\delta^2 + \beta\gamma){T_e}^2}{2} - \Omega^2 {T_e}^2/2$$

$$b_{11} = c\gamma\Omega {T_e}^2/2 \qquad b_{21} = -\gamma\Omega {T_e}^2/2$$

$$b_{12} = \left(cT_e\left(1 + \frac{(\alpha+\delta)T_e}{2}\right) - \frac{\beta {T_e}^2}{2}\right)\Omega$$

$$b_{22} = (-T_e + (c\gamma - 2\delta)\, {T_e}^2/2)\Omega$$

$$f_1 = 0.5c\gamma {T_e}^2 i_{s\beta} + cT_e{}^2\Omega\varphi_{r\alpha} + (cT_e\left(1 + \frac{(\alpha+\delta)T_e}{2}\right) - \beta {T_e}^2/2)\, \varphi_{r\beta}$$

$$f_2 = 0.5c\gamma {T_e}^2 i_{s\alpha} + cT_e{}^2\Omega\varphi_{r\beta} - (cT_e(1 + \frac{(\alpha+\delta)T_e}{2}) - \beta {T_e}^2/2)\, \varphi_{r\alpha}$$

$$f_3 = 0.5c\gamma {T_e}^2 i_{s\beta} - T_e{}^2\Omega\varphi_{r\alpha} + (0.5(c\gamma - 2\delta){T_e}^2 - T_e)\varphi_{r\beta}$$

$$f_4 = 0.5c\gamma {T_e}^2 i_{s\alpha} - T_e{}^2\Omega\varphi_{r\beta} - (0.5(c\gamma - 2\delta){T_e}^2 - T_e)\varphi_{r\alpha}$$

$$a_1 = aT_e(1 + \alpha T_e)/2 \qquad a_2 = a\gamma {T_e}^2/2$$

$$\sigma = 1 - \frac{{M_{sr}}^2}{L_s L_r} \qquad a = \frac{1}{\sigma L_s} \qquad b = 1/\sigma L_r$$

$$c = (1 - \sigma)/\sigma M_{sr} \qquad \alpha = (aR_s + \frac{c\, M_{sr} R_r}{L_r})$$

$$\beta = \frac{c\, R_r}{L_r} \qquad \gamma = \frac{M_{sr}\, R_r}{L_r} \qquad \delta = -\frac{R_r}{L_r}.$$

REFERENCES

1. Cheng M, Sun L, Buja G, Song L. Advanced Electrical Machines and Machine-Based Systems for Electric and Hybrid Vehicles. Energies. 2015; 8(9): 9541-9564. https://doi.org/10.3390/en809954.
2. Koengkan M, Fuinhas J.A, Teixeira M, Kazemzadeh E, Auza A, Dehdar F, Osmani F. The capacity of battery-electric and plug-in hybrid electric vehicles to mitigate CO_2 emissions: macroeconomic evidence from european union countries. World Electr. Veh. J. 2022:13-58. https://doi.org/10.3390/wevj13040058.
3. Ouamara D, Maidi A, Chaibet A, Boukhnifer M. Fault diagnosis techniques for electrical powertrain systems- Review. IEEE International Conference on applied automation and industrial diagnostics. 2019:

19229554. https://doi.org/10.1109/ICAAID.2019.8935003.
4. Boukhnifer M, Raisemche A. A fault tolerant control for induction motor in electrical vehicle. IEEE International Conference on Control Application. 2012;136-141. https://doi.org/10.1109/CCA.2012.6402663.
5. Chaibet A, Boukhnifer M, Ouddah N, Monmasson E. Experimental Sensorless Control of Switched Reluctance Motor for Electrical Powertrain System. Energies. 2020;13(12):3081. https://doi.org/10.3390/en1312308.
6. Rkhissi-Kammoun Y, Ghommam J, Boukhnifer M, Mnif F. Two current sensor fault detection and isolation schemes for induction motor drives using algebraic estimation approach. Mathematics and Computers in Simulation. 2019;157:39-62. https://doi.org/10.1016/j.matcom.2018.09.010.
7. Raisemche A, Boukhinfer M, Larouci C, Diallo D. Two Active Fault Tolerant Control shemes of induction motor drive in EV or HEV. IEEE Trans. Veh. Technol. 2014;63(1):19-29. https://doi.org/10.1109/TVT.2013.2272182.
8. Ouamara D, Boukhnifer M, Chaibet A, Maidi A, Sava A and Adjallah K. Fault detection and isolation current sensor of electrical powertrain system. 2020 International Conference on Control, Automation and Diagnosis (ICCAD). 2020:1-6. http://dx.doi.org/10.1109/ICCAD49821.2020.9260549.
9. Espinoza-Trejo DR, Campos-Delgado DU, Bossio G, Bárcenas E, Hernández-Díez JE, Lugo-Cordero LF. Fault diagnosis scheme for open-circuit faults in field-oriented control induction motor drives. IET Power Electronics. 2013;6(5):869-877. https://doi.org/10.1049/iet-pel.2012.0256.
10. Tallam RM. A survey of methods for detection of stator-related faults in induction machines. IEEE Transactions on Industry Applications.. 2007;43(4): 920-933. https://doi.org/10.1109/TIA.2007.900448.
11. Goh Y-J, Kim O. Linear Method for Diagnosis of Inter-Turn Short Circuits in 3-Phase Induction Motors. Applied Sciences. 2019;9(22):4822. https://doi.org/10.3390/app9224822.
12. Maraaba L, Al-Hamouz Z, Abido M. An efficient stator inter-turn fault diagnosis tool for induction motors Energies. 2018;11(3):653. https://doi.org/10.3390/en11030653.
13. Pietrowski W, Górny K. Detection of inter-turn short-circuit at start-up of induction machine based on torque analysis. Open Physics. 2017; 15 (1): 851-856. https://doi.org/10.1515/phys-2017-0101.
14. Vishwanath H, Maruthi G.S. Detection of stator winding inter-turn short circuit fault in induction motor using vibration signals by MEMS accelerometer. Electric Power Components and Systems Rao. 2017;45(13):1463-1473. https://doi.org/10.1080/15325008.2017.1358777.
15. Krzysztofiak M, Skowron M, Orlowska-Kowalska T. Analysis of the impact of stator inter-turn short circuits on PMSM drive with scalar and vector control. Energies. 2021;14(1):153. https://doi.org/10.3390/en14010153.
16. Almounajjed A, Sahoo AK, Kumar M.K Diagnosis of stator fault severity in induction motor based on discrete wavelet analysis. Measurement. 2021;182. https://doi.org/10.1016/j.measurement.2021.109780.
17. Diwatelwar KP, Malode SK. Fault detection and analysis of three-phase induction motors using MATLAB Simulink model. International Research Journal of Engineering and Technology (IRJET). 2018; 5(5): 1643-1649.
18. Goh YJ, Kim O. Linear method for diagnosis of inter-turn short circuits in 3-Phase induction motors. Applied Sciences. 2019;9(22):4822. https://doi.org/10.3390/app9224822.
19. Khayam Hoseini SR, Farjah E, Ghanbari T, Givi H. Extended Kalman filter-based method for inter-turn fault detection of the switched reluctance motors. IET Electric Power Applications. 2016; 10(8): 714–722. https://doi.org/10.1049/iet-epa.2015.0602.
20. El Sayed W, Abd El Geliel M, Lotfy A. Fault diagnosis of PMSG stator inter-turn fault using extended Kalman Filter and unscented Kalman filter. Energies. 2020; 13(11):2972. https://doi.org/10.3390/en13112972.
21. Rosero J, Cusido J, Espinosa AG, Ortega JA, Romeral L. Broken bearings fault detection for a permanent magnet synchronous motor under non-constant working conditions by means of a joint time frequency analysis. IEEE International Symposium on Industrial Electronics. 2007:3415-3419. https://doi.org/10.1109/ISIE.2007.4375165.
22. Biram M, Taibi D, Bessedik SA, Benkhoris M.F. Least square support vectors machines approach to diagnosis of stator winding short circuit fault in induction motor. Diagnostyka. 2020;21(4):35-41. https://doi.org/10.29354/diag/130283
23. Bachir S, Tnani S, Trigeassou J.C and Champenois G. Diagnosis by parameter estimation of stator and rotor faults occurring in induction machines. IEEE Transactions on Industrial Electronics. 2006; 53(3): 963-973. https://doi.org/10.1109/TIE.2006.874258
24. Bensaoucha S, Brik Y, Moreau S, Bessedik SA, Ameur A. Induction machine stator short-circuit fault detection using support vector machine. International journal for computation and mathematics in electrical and electronic engineering. 2021; 40 (3): 373-389. http://doi.org/10.1108/compel-06-2020-0208
25. Wolkiewicz M, Tarchała G, Orłowska-Kowalska T and Kowalski C.T. Online Stator Interturn Short Circuits Monitoring in the DFOC Induction-Motor Driv:e. in IEEE Transactions on Industrial Electronics. 2016;63(4):2517-2528. https://doi.org/10.1109/TIE.2016.2520902
26. Akhil Vinayak B, Anjali Anand K, Jagadanand G. Wavelet-based real-time stator fault detection of inverter-fed induction motor. IET Electric Power Applications. 2019. https://doi.org/10.1049/iet-epa.2019.0273
27. Simon D. Using nonlinear kalman filtring to estimate signals. embedded systems desigh. 2006;19(7):38-53.
28. Schwartz L, Stear E.A computational Comparaison of Several non Linear filters. IEEE Transaction on Automatic Control. February 1968;13:83-86. https://doi.org/10.1109/TAC.1968.1098800.
29. Gliga LI, Chafouk H, Popescu D, Lupu C. Diagnosis of a permanent magnet synchronous generator using the extended Kalman filter and the Fast Fourier Transform: 7th International Conference on Systems and Control (ICSC). 2018:65-70. https://doi.org/10.1109/ICoSC.2018.8587632.
30. Hilairet M, Diallo D, Benbouzid MEH. A self Reconfigurable and fault Tolerant Induction Motor Control Architecture for Hybrid Electric Vehicles. International Conference on Electrical machines. Greece. September 2006.
31. Hilairet M, Auger F, Darengosse C. Two efficient Kalman filters for flux and velocity estimation of

induction motors. 2000 IEEE 31st Annual Power Electronics Specialists Conference. 2000;2:891-896. https://doi.org/10.1109/PESC.2000.879932.
32. Zanardelli WG, Strangas EG, Aviyente A. Identification of intermittent electrical and mechanical faults in permanent-magnet AC drives based on time–frequency analysis. IEEE Transactions on Industry Applications. 2007;43(4):971-980. https://doi.org/10.1109/TIA.2007.900446.
33. Satpathi K, Yeap YM, Ukil A, Geddada N. Short-time Fourier transform based transient analysis of VSC interfaced point-to-point DC system. IEEE Transactions on Industrial Electronics. 2018;65(5): 4080-4091. https://doi.org/10.1109/TIE.2017.2758745.

Received 2022-09-21
Accepted 2023-02-16
Available online 2023-02-20

Dehbia OUAMARA, Ph.D. student in electrical engineering specialty modeling and design of electromagnetic systems at Mouloud Mammeri University of Tizi Ouzou, where she worked as temporary teacher. She received her B.S. and M.S. degrees in automation and control system in 2015 and 2017, respectively. Her scientific interests are centered on automatic, control and diagnosis of power train system applied for electrical vehicles.

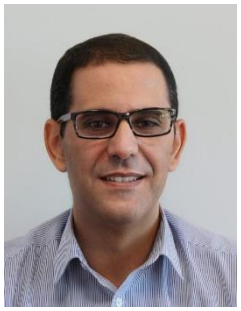

Moussa BOUKHNIFER (Senior Member, IEEE) received the M.Sc. degree in electrical engineering from the Institut National des Sciences Appliquées de Lyon, Lyon, France, in 2002, and the Ph.D. degree in control and engineering from the University of Orléans, Orléans, France, in December 2005. He received the habilitation for heading research (HDR Habilitation à Diriger des Recherches) from Paris Sud University, France, in December 2015. He is currently an Associate Professor HDR at Lorraine University, France. His main research interests are focused on energy management, diagnosis, and FTC control with its applications to electrical and autonomous systems. He is the author or coauthor of more than 100 scientific articles. He has served as the Chair of many international conferences and as an editorial member of many international journals. He is an Associate Editor of IEEE Transactions on Vehicular Technology journal.

Ahmed CHAIBET is an Associate Professor HDR at ISAT, University of Burgundy, France. He received the MSc degree in virtual reality and control of the complex systems from Versailles Saint-Quentin-en-Yvelines University, Versailles, France, in 2002 and the Ph.D. degree in control and engineering from the University of Évry Val-d'Essonne, Évry, France, in 2006. In Jully 2019, he received the «Habilitation à Diriger des Recherches» degree from the University of Paris XI. His main research interests and experience include advanced control techniques, diagnosis and fault tolerant control of autonomous vehicle and electric powertrains.

Ahmed MAIDI graduated in Automatic Control Engineering (State Engineer) from Hydrocarbons and Chemistry National Institute (INHC), Boumerdès, Algeria in 1997. He received his Magister in Electrical Engineering from M'Hamed Bougara, Boumerdès, Algeria in 2001. He obtained his PhD in Control Engineering from Mouloud Mammeri University, Tizi-Ouzou, Algeria in 2008 in collaboration with the Reaction and Process Engineering Laboratory, CNRS, ENSIC, Nancy, France. Currently, he is Professor in the Department of Automatic Control at Mouloud Mammeri University, Algeria. His primary research interests are
in modelling, simulation, optimisation and control of distributed parameter systems.